J Solid State Eletrochem (2004) 8: 422–429
DOI 10.1007/s10008-003-0475-8

ORIGINAL PAPER

Jacek Banaś · Urszula Lelek-Borkowska
Maria Starowicz

Electrochemical behaviour of p-Si in methanol solutions of chlorides

Received: 7 October 2003 / Accepted: 2 November 2003 / Published online: 4 March 2004
© Springer-Verlag 2004

Abstract The mechanism of anodic dissolutions of p-Si single crystals in CH_3OH–LiCl and CH_3OH–LiCl–HCl solutions was investigated by means of the following electrochemical methods: linear sweep voltammetry, the potentiostatic transient technique and XPS surface analysis. The dissolution of p-Si proceeds by a two-step mechanism with the creation of a Si(II) surface intermediate. At low anodic overvoltage the dissolution proceeds with the formation of porous silicon, probably through the reaction: $2Si(II) \rightarrow Si + Si(IV)$. Structural etching of the single crystal's surface was observed at high anodic overvoltage ($E > 2$ V). At this potential range, silicon dissolves with the formation of a Si(IV) soluble product. Electrolysis of the methanol solvent containing Si(IV) in the cell p-Si|CH_3OH–LiCl–Si(IV)|M, where M = Pt, Cu or 18/8 stainless steel, leads to the deposition of an amorphous organosilicon layer on the cathode. The analysis of the deposit performed by means of XPS, FTIR and SEM allows determination of the morphology and composition of the film. The layer consists of Si–OCH_3 compounds and can be created only in methanol solvent. The film is unstable in a humid atmosphere and undergoes transformation into a Si–OH layer.

Keywords Anodic dissolution · Cathodic deposition · Methanol · Silicon

Contribution to the 3rd Baltic Conference on Electrochemistry, Gdansk-Sobieszewo, Poland, 23–26 April 2003

Dedicated to the memory of Harry B. Mark, Jr. (28 February 1934–3 March 2003)

J. Banaś (✉) · U. Lelek-Borkowska · M. Starowicz
Department of General and Analytical Chemistry,
Faculty of Foundry Engineering,
AGH-University of Science and Technology,
ul. Reymonta 23, 30-059 Krakow, Poland
E-mail: jbs@agh.edu.pl

Introduction

The mechanism and kinetics of anodic dissolution of silicon are relatively well recognized in aqueous media, especially in fluoride and alkaline environments [1, 2, 3, 4, 5]. In our opinion, more attention should be paid to the electrochemical properties of silicon in organic solutions of electrolytes. Our investigation of metal dissolution and passivation in organic environments shows that these media give the possibility to control the passivation process by reducing or controlling the concentration of the passivating agent, the source of the oxygen necessary for oxide formation (water or oxyacid molecules) [18, 19, 20, 21, 22]. Organic solutions of electrolytes also enable control of the etching morphology of the metal surface, from polishing to structural etching, dependent on the dielectric permittivity and donor–acceptor properties of the solvent.

The first studies of the electrochemical properties of silicon in organic and mixed water–organic solutions were focused on the problem of oxide formation [6, 7, 8]. The effect of organic solvent addition (*N*,*N*-dimethylformamide, dimethyl sulfoxide or ethanol) on the morphology of pores growing in a silicon surface layer was also investigated [6, 7, 8, 9, 10, 11, 12, 13]. It was found that the pore diameter and morphology depend on the type of organic solvent additions [9]. Kohl and coworkers [14, 15, 16] investigated silicon behaviour in acetonitrile containing hydrogen fluoride or complex MF^{m-1} anions, which were the fluoride donors for the anodic reaction [16, 17]. They found that in these environments the silicon dissolves to give the tetravalent form without hydrogen evolution. The latter process is unwanted but inevitable in aqueous media. The mechanism of silicon dissolution was initiated, like in water, by hole consumption, which was followed by a few steps of electron injection [14]. Fluorine-containing ions like BF_4^-, PF_6^-, AsF_6^- and SbF_6^- were the source of the F^- ions necessary for Si(IV) complexation in fluoride-free solutions [16, 17]. The above-mentioned paper [14]

focuses on the mechanism of silicon dissolution. There is very little knowledge about the products of silicon dissolution in organic media. It is not clear if silicon exists in anolytes as an inorganic complex or as an organosilicon fluoride compound.

The aim of this study was to explain the mechanism of anodic dissolution in methanol solutions of chlorides. Also investigated was the cathodic deposition of the dissolved silicon product on the metal surface in this environment.

Experimental

Investigations were performed on boron-doped p-Si single-crystal wafers, with the crystallographic orientation (111) and (100). The resistance of the samples was 10 Ω cm^{-1}.

The metal/semiconductor junction was prepared by gold sputtering. The entire sample except for the electrode surface was isolated by silicon resin. Anhydrous methanol was obtained according to a published procedure [23]. The amount of water, evaluated by the Karl–Fischer method, was lower than 0.01%. CH_3OH–LiCl solutions were prepared by dissolution of anhydrous lithium chloride in anhydrous methanol. The mixing of CH_3OH–LiCl with appropriate amounts of anhydrous CH_3OH–0.1 M HCl allowed us to obtain the CH_3OH–LiCl–HCl solutions. CH_3OH–0.1 M HCl was obtained by bubbling dried gaseous HCl into anhydrous methanol. The concentration of HCl was established by estimation of the Cl^- content in solutions by means of atomic absorption spectroscopy.

A three-electrode system was used in the electrochemical measurements. The system was composed of a platinum auxiliary electrode, a reference electrode and a p-Si working electrode. An Ag|AgCl/Cl^-, methanol or an Ag|Ag^+, methanol electrode was used as the reference electrode. All the potential values were recalculated to the standard hydrogen electrode and these values are given in the paper. The investigations were performed at room temperature in deaerated solutions (Ar bubbling).

Linear sweep voltammetry (LSV) and the potentiostatic transient technique were used for evaluation of the polarization curves. LSV was obtained by means of PS-6 (Meinsberg, Germany) and Voltalab PGZ 301 (Radiometr Analytical, France) potentiostats.

Deposition of the organosilicon films was carried out in a p-Si|CH_3OH–LiCl–Si(IV)|M (M = Pt, Cu, 18/8 stainless steel) system. The deposition parameters were: i = 0.005 A/cm^2, E = −1.40 V. The film after deposition was rinsed in anhydrous methanol.

The morphology of the etched surface as well as of the deposited film was investigated by means of X-ray photoelectron spectroscopy (XPS) and scanning electron microscopy (SEM) with an EDS analyzer. XPS measurements were performed using a ESCA-VSV spectrometer. Mg Kα X-rays of 1253.6 eV were used. SEM pictures were taken with the use of a JEOL 5500 LV electron microscope.

The composition of the deposited films was examined by Fourier transform infrared spectroscopy (FTIR) using a EPS-60 spectrometer with a beam condenser.

Results and discussion

Anodic dissolution of p-Si in methanol–chloride solutions

Silicon undergoes anodic dissolution in CH_3OH–LiCl. Figure 1 presents anodic polarization curves for p-Si(100) in 0.1 M LiCl in methanol. Dissolution of Si proceeds by a two-step mechanism. Figure 2 shows LSV

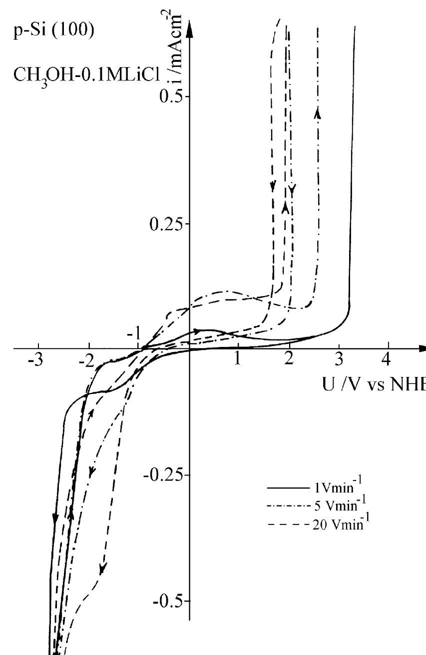

Fig. 1 LSV polarization curves for p-Si(100) in CH_3OH–0.1 M LiCl solution

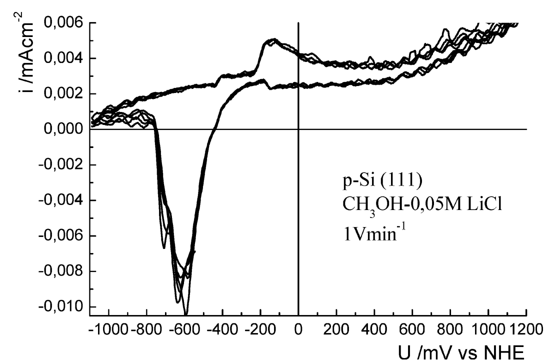

Fig. 2 LSV polarization curves for p-Si(111) in CH_3OH–0.05M LiCl solution

curves for the anodic polarization of silicon(111) in CH_3OH–0.05 M LiCl. Two anodic peaks are visible, the first at a potential of −0.4 V, the second at −0.1 V. The first peak is connected with the formation of divalent silicon, the second one with its oxidation to Si(IV). Two stages of anodic dissolution have been confirmed during potentiostatic transient experiments (Fig. 4a–c). There are two peaks in the transients curves with a potential impulse higher than 0.70 V imposed on the constant potential of −0.50 V. For the first LSV peak, dlog i/dlog[Cl^-] is 0.65 (Fig. 3). This value is similar to dlog i/dlog[F^-] equal to 0.57 obtained in aqueous solutions [13], which suggests a similar mechanism of reaction in water. The reaction order lower than 1.0 shows that the methanol molecules participate in the formation of the Si(II) product at low overvoltage. The confirmation of this process is the presence of oxygen in the form of O–Si(II) species as well as Si–OCH_3 groups in the surface layer (Fig. 5a, b). In the O 1s spectra, two signals

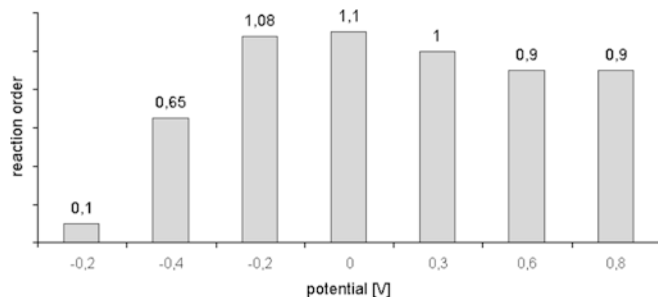

Fig. 3 The reaction order dlog i/dlog[Cl^-] as a function of potential

from oxygen are observed: the first at a binding energy $E_B = 532$ eV (O–Si(II) species), the second at $E_B = 533$ eV (O–Si(IV) species) [24]. The XPS spectra of Si 2p show, according to this assumption, that signals from Si(II) and Si(IV) forms are visible [24]. In the range of the C 1s band, three peaks are observed: at $E_B = 284.6$ eV (carbon in C–C or C–H bonds) [27, 28], at $E_B = 286.5$ eV (C–O) [25] and at $E_B = 288.4$ eV, which comes from C in Si–OCH_3 species [26].

The presence of Si(II) at higher anodic overvoltages, confirmed by XPS measurements, is probably connected with incomplete activation of the silicon surface during the dissolution in the transpassive range (see Fig. 8c–f). Some areas of the surface are covered with surface product Si(II) and some undergo active dissolution, with the formation of Si(IV). Nonetheless, the ratio Si(II)/Si(IV) decreases with increasing potential because of the increase of the active surface.

Methanol molecules undergo rapid electrosorption on a silicon surface and form a –$SiOCH_3$ film. The film is thermodynamically stable below the potential of methanol oxidation. The thermodynamic value of the equilibrium potential of the reaction:

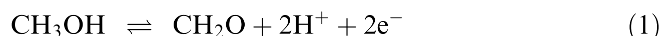

$$CH_3OH \rightleftharpoons CH_2O + 2H^+ + 2e^- \quad (1)$$

equals 0.3 V (SHE). The oxidation of methanol and methoxy surface products is obviously a very complicated multi-step mechanism, strongly dependent on the kind and concentration of the surface defects and on the crystallographic orientation of the electrode material [19, 20, 21, 22]. Thus the removal of methoxy groups from the silicon layer by their oxidation can be characterized by the potential range and not by the definite potential value. Anyway, below a potential of ~0.30 V, methanol particles take part in the first step of an anodic reaction and participation of chloride ions is probably limited to the second step of the oxidation:

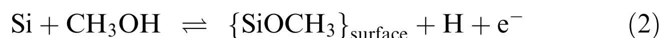

$$Si + CH_3OH \rightleftharpoons \{SiOCH_3\}_{surface} + H + e^- \quad (2)$$

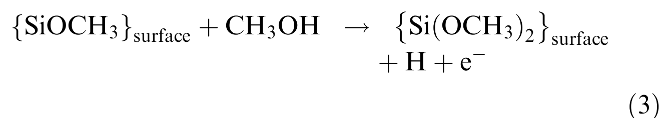

$$\{SiOCH_3\}_{surface} + CH_3OH \rightarrow \{Si(OCH_3)_2\}_{surface} + H + e^- \quad (3)$$

$$\{SiOCH_3\}_{surface} + Cl^- \rightarrow \{Si(OCH_3)Cl\}_{sol} + e^- \quad (4)$$

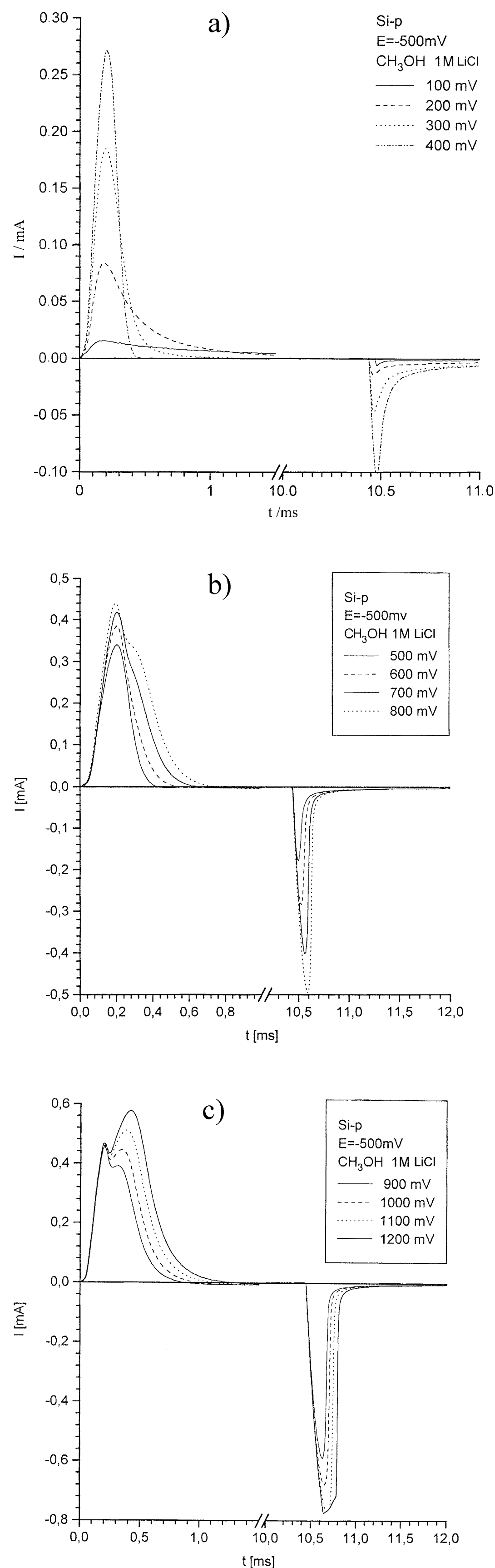

Fig. 4 Potentiostatic transients on p-Si in CH_3OH–1 M LiCl solution

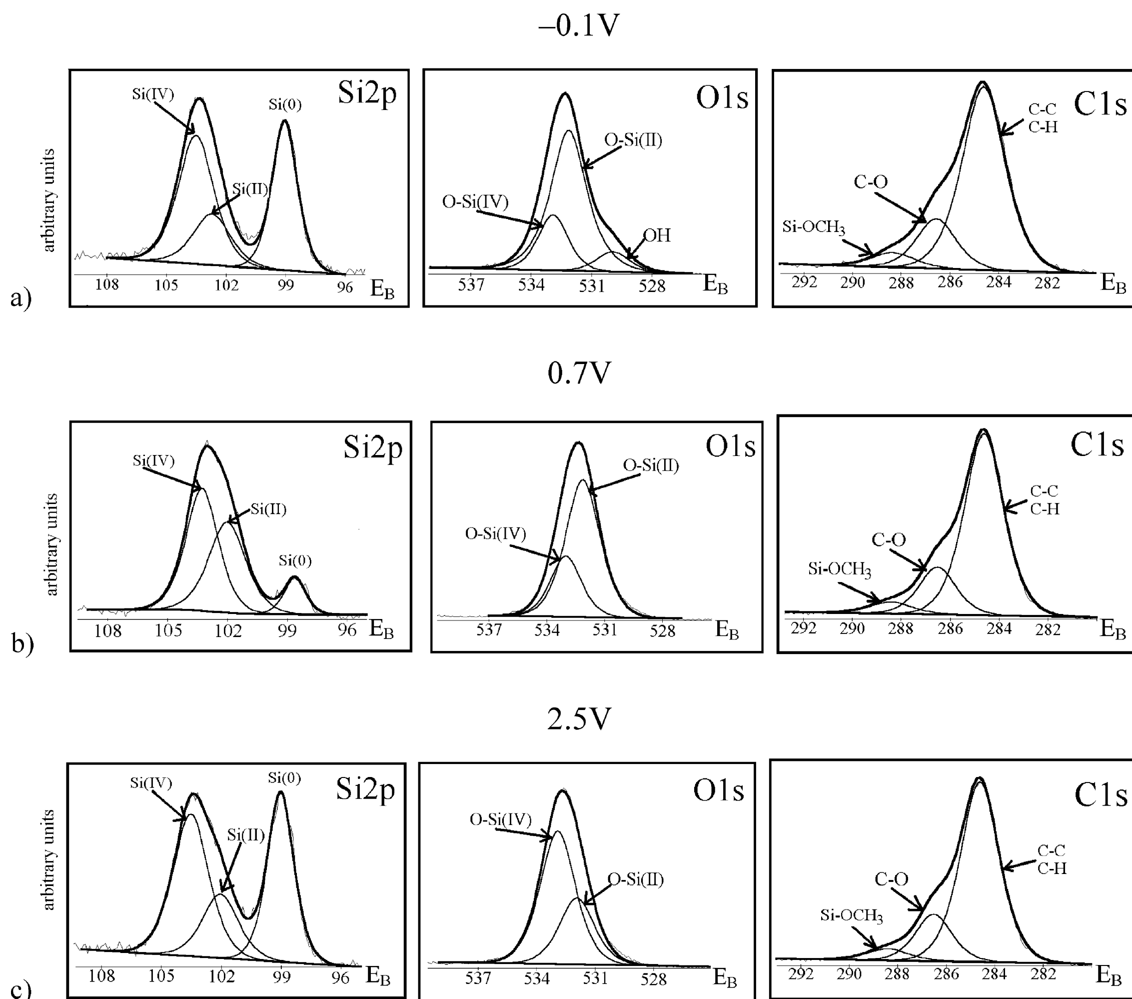

Fig. 5 XPS spectra in the Si 2p and O 1s ranges for the silicon surface etched in CH_3OH–LiCl solution: (**a**) at a potential of −0.1 V; (**b**) at a potential of 0.7 V; (**c**) at a potential of 2.5 V

The reaction order dlog i/dlog$[Cl^-]=0.65$ suggests that chloride ions participate in the formation of soluble compounds according to Eq. 4 (Fig. 3).

Silicon single crystals etched at a potential of −0.15 V show a lot of pores growing in a determined direction (111). The surface is covered with a black deposit. In our opinion, the formation of porous silicon in the potential range of stability of Si(II) compounds is probably connected with a dismutation reaction:

$$2\mathrm{Si(II)} \rightarrow \mathrm{Si} + \mathrm{Si(IV)} \quad (5)$$

At the potential of the current plateau the layer becomes thick and the amount of Si(II) increases (Fig. 5b).

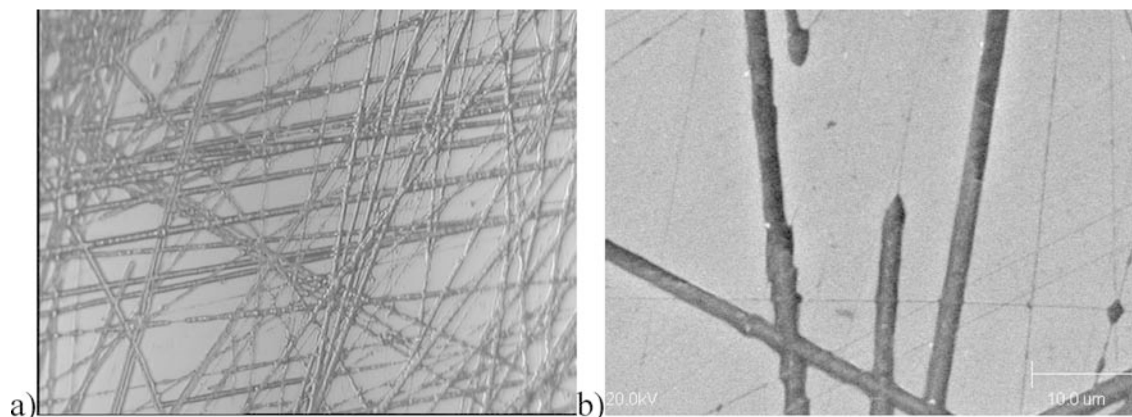

Fig. 6 Surface of p-Si(111) etched in CH_3OH–LiCl solution at a potential of 2.5 V for 15 min: (**a**) magnification 260×; (**b**) magnification 2500×

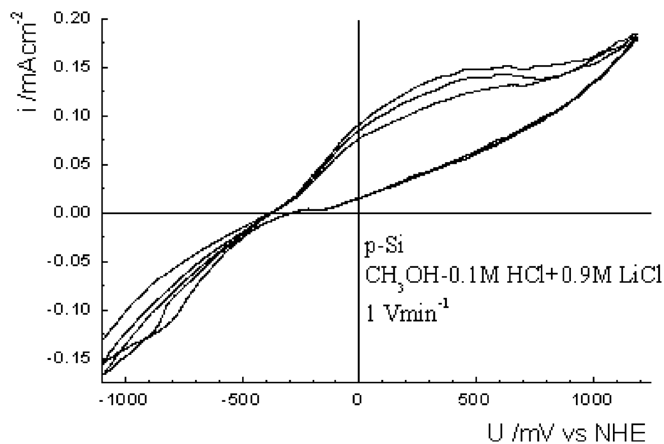

Fig. 7 LSV polarization curves for p-Si(111) in CH_3OH–HCl + LiCl solution

At the transpassive potential of 2.5 V, dissolution becomes very fast and the anodic film is thin and contains mostly tetravalent silicon (Fig. 5c). Also at high anodic potentials, very small signals in the Cl 2p band were observed, which suggests that chloride ions participate only in the formation of the soluble product, but not in the formation of the surface film. In this potential range, chloride ions play a dominant role in the complexation process (complexing of Si(IV)). The reaction order dlog i/dlog[Cl^-] at high anodic overvoltage is close to 1.0 (Fig. 3). The dissolution process in this potential range can be expressed as follows:

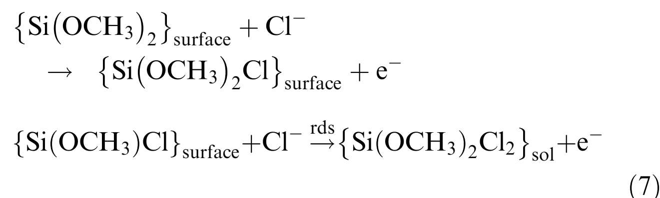

$$\{Si(OCH_3)_2\}_{surface} + Cl^- \rightarrow \{Si(OCH_3)_2Cl\}_{surface} + e^-$$

$$\{Si(OCH_3)Cl\}_{surface} + Cl^- \xrightarrow{rds} \{Si(OCH_3)_2Cl_2\}_{sol} + e^- \quad (7)$$

The surface image after the anodic treatment shows that silicon undergoes etching in the transpassive range of potentials (> 2.5 V) and dissolution starts on the surface imperfections (Fig. 6a, b).

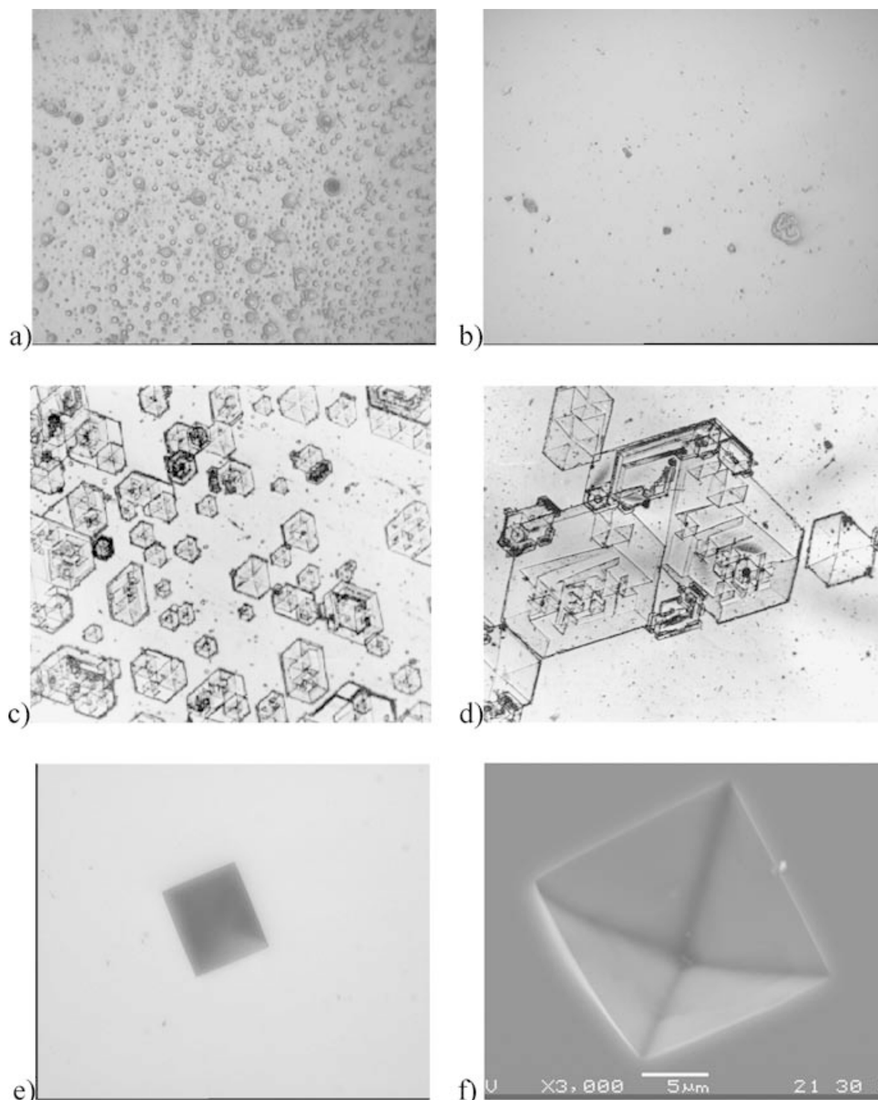

Fig. 8 Surface of p-Si etched in CH_3OH–HCl solution at potentials of: (**a**) −0.15 V for 5 h; (**b**) 0.7 V for 5 h; (**c**) 2.5 V for 15 min (100); (**d**) 2.5 V for 20 min (magnification 400×); (**e**) 2.5 V for 15 min (111) (magnification 560×); (**f**) 2.5 V for 15 min (111) (SEM pictures)

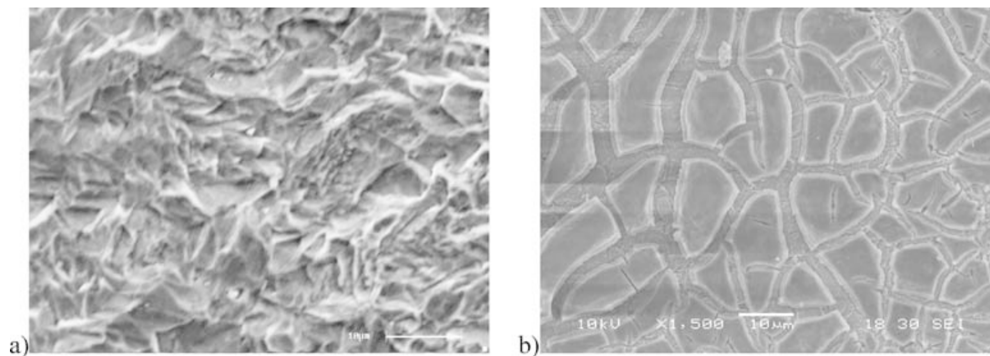

Fig. 9 Films deposited on stainless steel 18/8: (**a**) thin; (**b**) thick

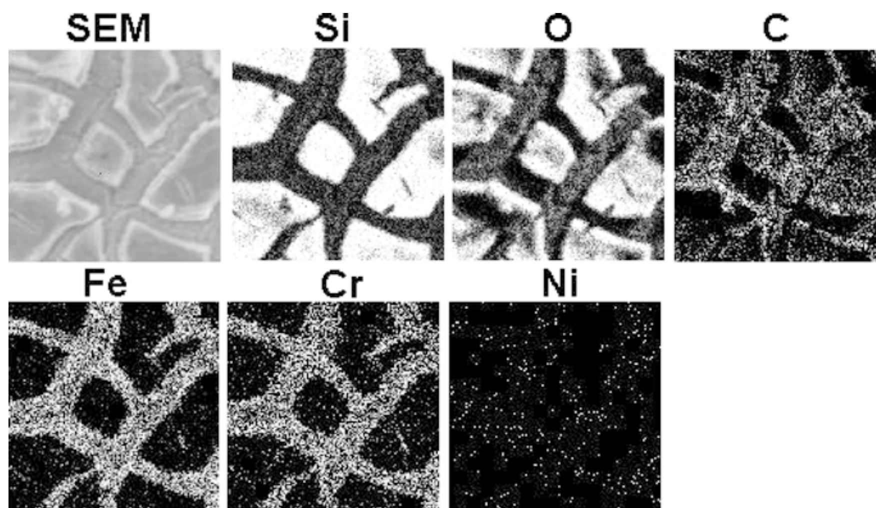

Fig. 10 Distribution of elements in the deposited layer

Dissolution of silicon in methanol containing hydrochloride (CH_3OH–LiCl–HCl, $[Cl^-]=1$ M) proceeds more intensively (Fig. 7). There is only one wide peak visible on the anodic curve. The first anodic peak, connected with the formation of the $Si(OCH_3)_2$ compound, practically disappears. The second anodic peak is much higher and its maximum is shifted to more positive values (+0.40 V) compared to CH_3OH–LiCl solutions. This means that the presence of hydrogen ions stimulates removal of the $Si(OCH_3)_2$ compound and facilitates formation of the soluble product $Si(OCH_3)_2Cl_2$.

A high rate of dissolution of p-Si in CH_3OH–LiCl–HCl was confirmed by surface morphology investigations (Fig. 8a–f). Silicon single crystals etched at a potential of −0.15 V show a lot of pores growing in a determine direction (100) (Fig. 8a). At the potential of the current plateau, after the anodic peak (0.7 V), the surface is evenly etched (Fig. 8b). At the transpassive potential (over 2.5 V), dissolution becomes anisotropic and the surface morphology depends on the crystallographic orientation (Fig. 8c–f).

Cathodic deposition of organosilicon films

The soluble product of the anodic dissolution of silicon in CH_3OH–LiCl undergoes deposition on a catholically polarized metal surface. We performed investigations of the morphology and chemical composition of the deposited film on Pt, Cu and a 18/8 stainless steel surface. These metals have been chosen because of their relatively high corrosion resistance in the investigated solutions and is why metal dissolution processes could be avoided. The deposition procedure was presented in the experimental section. Figure 9 shows the cathodic deposit on stainless steel. Similar deposits were obtained on the other metal cathodes. The thin films, deposited in a short period of time, are homogenous and evenly distributed (Fig. 9a). Thick films undergo cracking during the aging process (Fig. 9b).

The electron diffraction surface analysis (EDSA) shows that the deposited films consist of silicon, oxygen and carbon (Fig. 10). The image of the elements' distribution shows that the loci of silicon and oxygen atoms cover spaces between the cracks. Atoms of the metal substrate (Fe, Cr, Ni) can be observed in the gaps and their distribution looks like a negative of image of the Si and O distributions.

Figure 11 shows XPS spectra of the film deposited on a Pt electrode: the Si 2p band (Fig. 11a), the C 1s band (Fig. 11b) and the O 1s band (Fig. 11c). XPS spectra of the Si 2p band indicate the presence of only one form of silicon, Si(IV) ($E_B=103.1$ eV) (Fig. 11a) [29]. The XPS spectrum of the C 1s band (Fig. 11b) shows three peaks with binding energies of 284.7, 286.6 and 288.5 eV. The

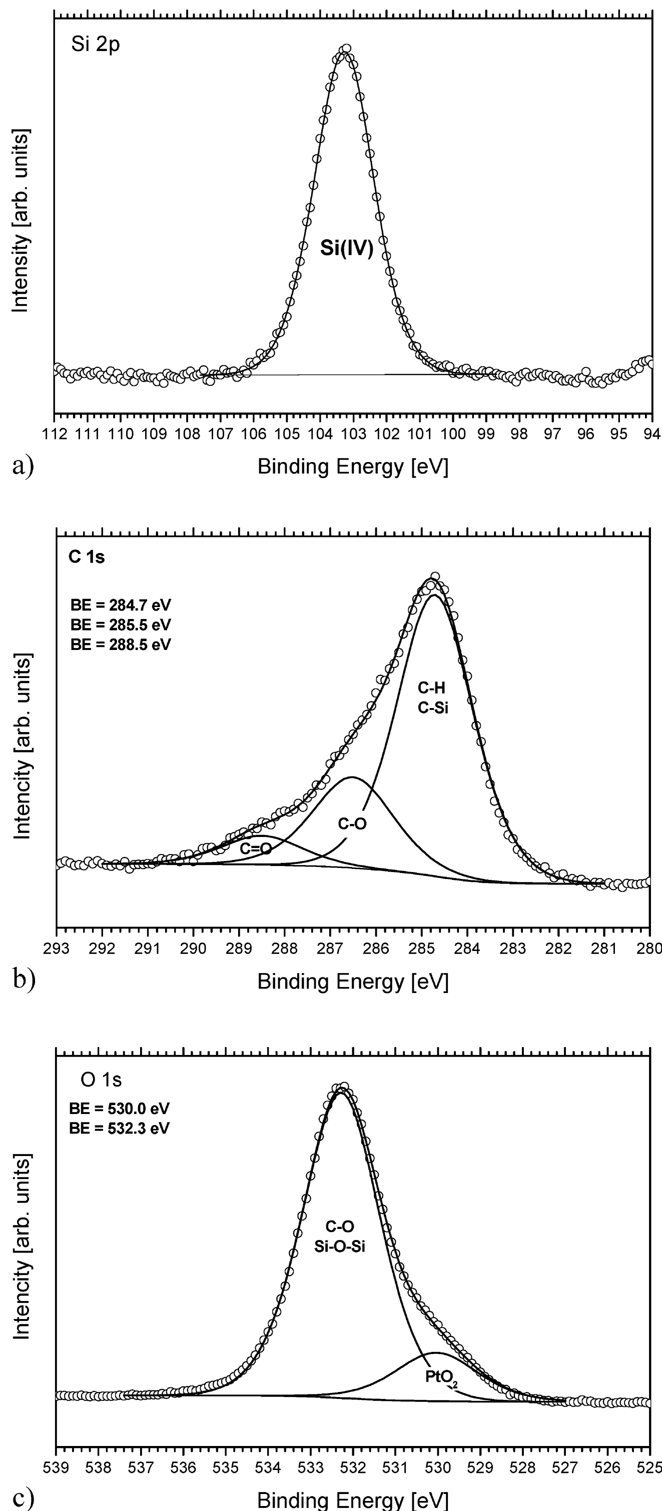

Fig. 11 XPS spectrum: (**a**) Si 2p band; (**b**) C 1s band; (**c**) O 1s band

first peak is connected with the presence of carbon in a C–H bond. The second peak indicates C–O bonds in methanol. The third one refers to carbon double bonded to oxygen [29]. The peaks in the O 1s spectrum (Fig. 11c) stem from two forms of oxygen: metal oxides ($E_B = 530.0$ eV) and organic compounds containing

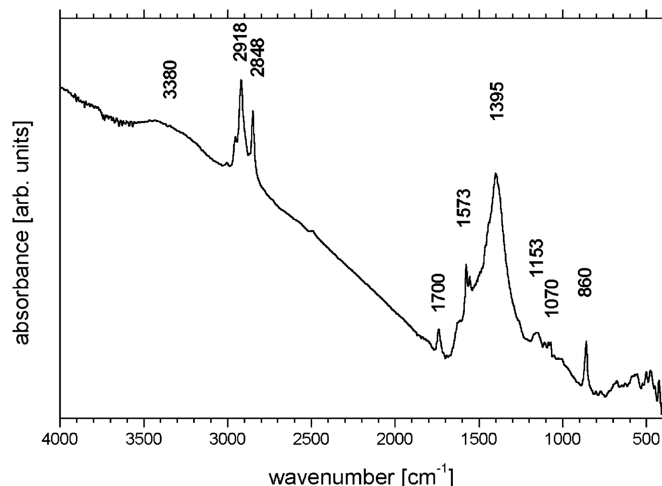

Fig. 12 FTIR spectrum of fresh film deposited on Pt

oxygen atoms ($E_B = 532.3$). The second value of the binding energy can be also attributed to Si–O species [29].

FTIR measurements were carried out on the fresh film shortly after deposition and on the layer aged for one week. Figure 12 shows the spectrum of a fresh layer deposited on Pt. Signals with wave numbers of 3000–2800 cm^{-1} and a sharp peak at 1395 cm^{-1} are characteristic for CH_3 and CH_2 groups [30]. The maximum at 1410 cm^{-1} can stem from Si–CH_2–Si connections as well as from the compound SiO_2. Because of the high intensity of the 1395 cm^{-1} signal, the existence of both compounds can be assumed. The peak at 859 cm^{-1} is connected with Si–OCH_3 compounds. Weak signals at 1070 and 1153 cm^{-1} probably stem from Si–O–Si and Si–O–CH_3 groups or from the C–OH bond in methanol [30]. The maximum at 1700 cm^{-1} is a result of oscillations of the C = O double bond in the carboxylic group. The weak signal at 1573 cm^{-1} and wide but weak band with wavenumbers in the range 3600–3400 cm^{-1} indicate that molecules of water are present in the layer.

Figure 13 presents the FTIR spectrum of aged film. The main difference between the spectrum of the aged layer and the fresh film is a very intensive peak at 1088 cm^{-1}. This points to the presence of large amounts of Si–O–Si chains. The signals at 800 cm^{-1} and 460 cm^{-1} are also responsible for Si–O bonds. In addition, there is a peak visible at 950 cm^{-1}, which indicates the presence of Si–OH species [30].

The presented investigations show that cathodic polarization of a metal surface in CH_3OH–LiCl solutions containing dissolved Si(IV) leads to the deposition of organosilicon compounds. The deposition proceeds in the potential range of methanol reduction. The deposited amorphous layer is composed mainly of Si–O–Si and Si–OCH_3 groups, but some Si–CH_2–Si and Si–CH_3 species are present in the film. The mechanism of the deposition is not clear. It seems that a high concentration of –OCH_3 produced on the cathode facilitates bonding and deposition of methoxysilicon species, which

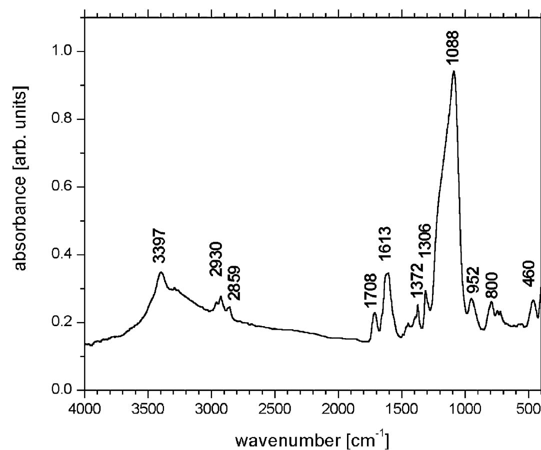

Fig. 13 FTIR spectrum of aged film on Pt

undergoes, under open-air conditions, hydrolysis and condensation according to the scheme:

$$\equiv \mathrm{Si - OCH_3} + \mathrm{H_2O} \rightarrow \equiv \mathrm{Si - OH} + \mathrm{CH_3OH} \quad (8)$$

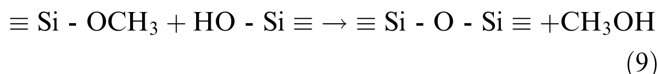

$$\equiv \mathrm{Si - OCH_3} + \mathrm{HO - Si} \equiv \rightarrow \equiv \mathrm{Si - O - Si} \equiv + \mathrm{CH_3OH} \quad (9)$$

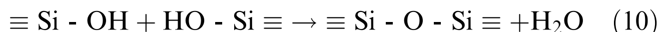

$$\equiv \mathrm{Si - OH} + \mathrm{HO - Si} \equiv \rightarrow \equiv \mathrm{Si - O - Si} \equiv + \mathrm{H_2O} \quad (10)$$

The reactions in the Eqs. 8, 9, 10 are similar to those observed in sol–gel techniques of silica deposition [30].

Conclusions

Anodic dissolution of p-Si in anhydrous methanol solutions of chlorides proceeds in two consecutive steps via a Si(II) surface intermediate. At low overvoltage the formation of "porous silicon" was observed during anodic dissolution.

In the range of medium anodic overvoltage the silicon surface is covered by a relatively stable film of $Si(II)_{ad}$ compounds. At high overvoltage the anodic dissolution starts on the defects of the single crystal surface and structural etching of the silicon surface can be observed. The dissolution proceeds with the formation of a Si(IV) soluble product. This soluble product can be deposited on the metal surface in the course of cathodic polarization. The deposited film consists mainly of $Si–OCH_3$ and Si–O–Si compounds. This layer is unstable and undergoes transformation into a Si–O–Si amorphous film.

References

1. Turner DR (1958) J Electrochem Soc 105:402
2. Memming R, Schwandt G (1966) Surf Sci 4:109
3. Lehmann V, Föll H (1987) J Electrochem Soc135:2831
4. Lévy-Clément C, Lagoubi A, Tenne R, Neumann-Spallart M (1992) Electrochim Acta 37:877
5. Allongue P, Costa-Kieling V, Gerischer H (1993) J Electrochem Soc 140:1018
6. Schmidt PF, Michel W (1957) J Electrochem Soc 104:230
7. Croset M, Petreanu E, Samuel D, Amsel G, Nadai JP (1971) J Electrochem Soc 118:717
8. Madou MJ, Gomes WP, Fransen F, Cardon F (1982) J Electrochem Soc 129:2749
9. Lust S, Lèvy–Clèment C (2000) Phys Status Solidi A 182:17
10. Hasse G, Christophersen M, Carstensen J, Föll H (2000) Phys Status Solidi A 182:23
11. Christophersen M, Carstensen J, Föll H (2000) Phys Status Solidi A 182:561
12. Christophersen M, Merz P, Quenzer J, Carstensen J, Föll H (2000) Phys Status Solidi A 182:103
13. Christophersen M, Carstensen J, Feuerhake A, Föll H (2000) Mater Sci Eng B 69–70:194
14. Propst EK, Kohl PA (1994) J Electrochem Soc 141:1006
15. Rieger MM, Kohl PA (1995) J Electrochem Soc 142:1490
16. Flake JC, Rieger MM, Schmid GM, Kohl PA (1999) J Electrochem Soc 146:4485
17. Rieger MM, Flake JC, Kohl PA (1999) J Electrochem Soc 146:1960
18. Banaś J (1987) Electrochim Acta 32:871
19. Banaś J (1990) Metall Foundry Eng 16:73
20. Banaś J, Mazurkiewicz B, Stypua B (1992) Electrochim Acta 37:1069
21. Banaś J, Stypua B, Mazurkiewicz B (1992) Metall Foundry Eng 18:191
22. Banaś J (1995) Mater Sci Forum 185–188:845
23. Vogel AI (1984) Preparatyka organiczna. WNT, Warsaw
24. Hollinger G (1981) Appl Surf Sci 8:318
25. Clark DT, Thomas HR (1978) J Polym Sci Polym Chem Ed 16:791
26. Laoharojanaphand P, Lin TJ, Stoffer JO (1990) J Appl Polym Sci 40:369
27. Sundberg P, Larsson R, Folkesson B (1988) J Electron Spectrosc Relat Phenom 46:19
28. Brown NMD, Hewitt JA, Meenan B Jr (1992) Surface Interface Anal 18:187
29. Starowicz M (2003) Doctoral thesis. AGH-University of Science and Technology, Krakow, Poland
30. Martinez JR, Ruiz F, Vorobiev ZV, Perz F, Gonzalez-Hernandez J (1998) J Chem Phys 109:7511